Int. J. Heat Mass Transfer. Vol. 29, No. 12, pp. 1855–1868, 1986
Printed in Great Britain

0017–9310/86 $3.00 + 0.00
Pergamon Journals Ltd.

Outward phase change in a cylindrical annulus with axial fins on the inner tube

P. V. PADMANABHAN and M. V. KRISHNA MURTHY

Refrigeration and Airconditioning Laboratory, Department of Mechanical Engineering, Indian Institute of Technology, Madras 600 036, India

(*Received* 18 *February* 1985 *and in final form* 10 *September* 1985)

Abstract—A theoretical analysis is presented for the phase change process occurring in a cylindrical annulus in which rectangular, uniformly spaced axial fins, spanning the annulus, are attached to the inner isothermal tube, while the outer tube is kept adiabatic. The model assumes conduction to be the only mode of heat transfer. The governing equations are solved by finite-difference methods. The time-wise evolution of the interface profile, phase-change fraction and energy stored/discharged and the effect of all the nine prescribable parameters are presented here. Based on the analysis a working formula

$$VF = 1.1275(Fo\ Ste\ T_f)^{0.624}(N)^{0.028}(L)^{-1.385}(W)^{-0.049}$$

is suggested for engineering design purposes.

INTRODUCTION

LATENT heat thermal energy storage (LHTES) systems employing phase-change materials (PCM) suffer from certain inherent handicaps. PCMs used in LHTES, are in general poor thermal conductors. During the energy discharge process, PCM freezes on to the heat transfer surfaces and acts as a self-insulator. The technique of adding crystallising and thickening agents to the PCM to alleviate the problems of supercooling and phase segregation, can further significantly reduce heat transfer by lowering the thermal conductivity of PCM and inhibiting convective motion in liquid PCM.

Heat transfer in LHTES devices can be enhanced by the following techniques:

(i) Mechanically scraping off the frozen PCM from heat transfer surfaces [1] or rotating the PCM container at slow speeds to prevent the frozen PCM from adhering to the heat transfer surfaces [2].
(ii) Using direct contact heat exchangers [3–8].
(iii) Microencapsulation of PCM [9–12].
(iv) Using extended surfaces [13–21].

The last mentioned technique forms the topic of investigation in the present paper. While there are a number of experimental investigations on freezing/melting of PCM bounded by finned surfaces in rectangular geometries [13–15] and cylindrical geometries [16–20], theoretical investigations are very few and are available mainly for rectangular geometries [13, 14, 21, 22].

There does not seem to be any theoretical study on the transient heat transfer process during the freezing/melting of PCM with fins in cylindrical geometries, the lone exception being the simplified model presented by Abhat *et al.* [23]. Outward phase change in an axially finned annulus is theoretically investigated in this paper. For the sake of clarity, the analysis and presentation of results are couched in terms of freezing but are valid for melting also.

STATEMENT OF THE PROBLEM

The PCM is contained in a cylindrical annulus with N rectangular fins parallel to the axis of the cylinder and evenly distributed around its circumference. The PCM-finned tube assembly is initially at a uniform temperature T^*_{in} which is different from the phase-change temperature T^*_f of the PCM. The outer circumference of the annular space is kept insulated. The inner circumference is subjected to a step change in temperature and maintained isothermal thereafter at T^*_w. If $T^*_w > T^*_f \geqslant T^*_{in}$ melting of the PCM will take place and for $T^*_w < T^*_f \leqslant T^*_{in}$ freezing will ensue. The phase-change process is sought to be accelerated by the addition of fins.

A schematic of the physical model for a unit cell bounded by two adjacent fins and the inner and outer cylindrical surfaces is shown in Fig. 1.

The model assumes one-dimensional conduction through the fin and two-dimensional conduction through the PCM. All the thermophysical properties are assumed to be independent of temperature. Natural convection in liquid PCM is ignored. The surfaces of the two adjacent fins constituting the boundaries for the unit cell are specified by the angle $\phi^* = \pm\beta^*(r^*)$ where β^* is given by the equation

$$\beta^* = \pi/N - \sin^{-1}(W^*/2r^*). \quad (1)$$

The problem can be mathematically described by the following set of equations.

NOMENCLATURE

AF heat transfer area factor, equation (38)
AFC, AFR, $APRZ$ coefficients defined in equations (23), (22), (17)
a thermal diffusivity
c specific heat
E^* normalisation quantity for energy components, equation (28)
$E1, E2, \ldots, E6$ energy density components, equations (29)–(34)
ET total energy density, equation (35)
EM maximum possible energy density, equation (36)
F, FR, FRR coefficients defined in equations (19)–(21)
FC fin content defined in equation (37)
Fo Fourier number, $a_1 t/r_w^{*2}$
Δh latent heat of phase change
L^* radial length of the fins
L dimensionless fin length, L^*/r_w^*
N total number of fins around the circumference
PFo, PR, PRR, PRZ, PZ, PZZ coefficients defined in equations (12)–(16), (18)
p root of Neumann's transcendental equation (41)
R, RF defined in equations (24), (25)
r^* radial coordinate
r dimensionless radius, $(r^*-r_w^*)/r_w^*$
Ste Stefan number, $\pm c_1(T_{in}^*-T_w^*)/\Delta h$
T^* temperature
T dimensionless temperature, $(T^*-T_w^*)/(T_{in}^*-T_w^*)$
t time
VF volume of melt/frozen fraction defined in equation (39)
W^* fin thickness
W dimensionless fin thickness, W^*/r_w^*.

Greek symbols
α^* half fin angle, $\sin^{-1}(W^*/2r^*)$
β^* half PCM angle, $(\pi/N-\alpha^*)$
η transformed radial coordinate $= r/r_f$ for phase 1 of PCM $= (r-L)/(r_f-L)$ for phase 2 of PCM
λ thermal conductivity
ρ mass density
ϕ^* angular coordinate
ϕ dimensionless angular coordinate, ϕ^*/β^*.

Subscripts
F fin
Fp fin portion adjoining phase p of PCM
f melt/freeze front
p phase p of PCM (1 = inner phase; 2 = outer phase)
w inner wall surface.

Superscript
* dimensional quantity.

Governing equation for PCM:

$$\frac{\partial^2 T_p^*}{\partial r^{*2}}+\frac{1}{r^*}\frac{\partial T_p^*}{\partial r^*}+\frac{1}{r^{*2}}\frac{\partial^2 T_p^*}{\partial \Phi^{*2}}=\frac{1}{a_p}\frac{\partial T_p^*}{\partial t} \quad (2a)$$

in $-\beta^* \leqslant \Phi^* \leqslant \beta^*$, $p=1$ in $r_w^* \leqslant r^* \leqslant r_f^*$

$p=2$ in $r_f^* \leqslant r^* \leqslant (r_w^*+L^*)$.

Governing equation for the upper fin:

$$\frac{\partial^2 T_{Fp}^*}{\partial r^{*2}}+\frac{1}{r^*}\frac{\partial T_{Fp}^*}{\partial r^*}\frac{(\alpha^*-\tan\alpha^*)}{\alpha^*} = \frac{1}{a_F}\frac{\partial T_{Fp}^*}{\partial t}+\frac{\lambda_p}{\lambda_F}\frac{\sec^2\alpha^*}{\alpha^*}\frac{1}{r^{*2}}\frac{\partial T_p^*}{\partial \phi^*}\bigg|_{\phi^*=\beta^*} \quad (2b)$$

$p=1$ in $r_w^* \leqslant r^* \leqslant r_f^*$

$p=2$ in $r_f^* \leqslant r^* \leqslant (r_w^*+L^*)$.

Boundary conditions:

—at the fin surface

$$T_p^* = T_{Fp}^* \text{ at } \phi^* = \pm\beta^*, \quad p=1 \text{ in } r_w^* \leqslant r^* \leqslant r_f^* \quad p=2 \text{ in } r_f^* \leqslant r^* \leqslant (r_w^*+L^*) \quad (2c)$$

—at the insulated boundary

$$\frac{\partial T_{Fp}^*}{\partial r^*}=0 \text{ at } r^*=(r_w^*+L^*) \quad (2d)$$

$$\frac{\partial T_2^*}{\partial r^*}=0 \text{ at } r^*=(r_w^*+L^*), \quad -\beta^* \leqslant \phi^* \leqslant \beta^* \quad (2e)$$

—at the inner tube wall surface

$$T_1^* = T_w^* \text{ at } r_w^*, \quad -\beta^* \leqslant \phi^* \leqslant \beta^* \quad (2f)$$

$$T_{F1}^* = T_w^* \text{ at } r^*=r_w^* \quad (2g)$$

—at the melt/freeze front

$$T_1^* = T_2^* = T_f^* \text{ at } r^*=r_f^*, \quad -\beta^* \leqslant \phi^* \leqslant \beta^* \quad (2h)$$

$$\left(\lambda_2\frac{\partial T_2^*}{\partial r^*}-\lambda_1\frac{\partial T_1^*}{\partial r^*}\right)\left[1+\frac{1}{r_f^{*2}}\left(\frac{\partial r_f^*}{\partial \phi^*}\right)^2\right]=\pm\rho_1\Delta h\frac{\partial r_f^*}{\partial t}$$

at

$$r^*=r_f^*, \quad -\beta^* \leqslant \phi^* \leqslant \beta^* \quad (+ \text{ melting}, - \text{ freezing}). \quad (2i)$$

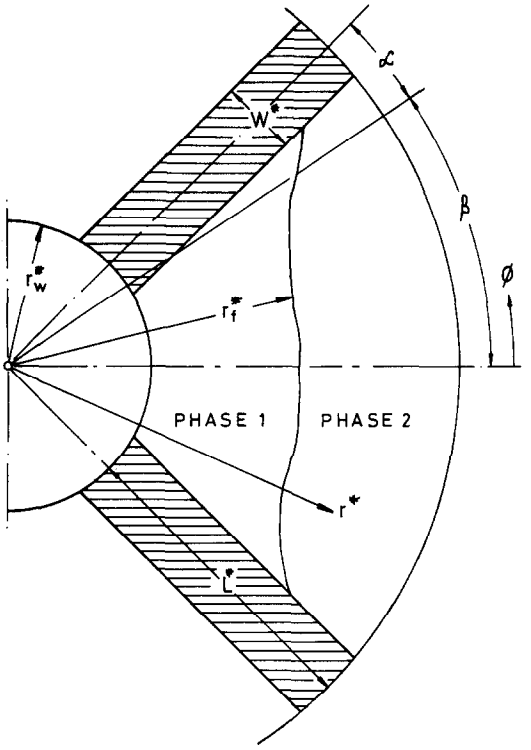

FIG. 1. Physical model and coordinate system.

Initial conditions:

$$T^*_{F2} = T^*_{in} \text{ in } r^*_w \leqslant r^* \leqslant (r^*_w + L^*) \quad (2j)$$

$$T^*_2 = T^*_{in} \text{ in } r^*_w \leqslant r^* \leqslant (r^*_w + L^*), \quad -\beta^* \leqslant \phi^* \leqslant \beta^* \quad (2k)$$

$$r^*_f = r^*_w \text{ in } -\beta^* \leqslant \phi^* \leqslant \beta^*. \quad (2l)$$

It is very difficult to obtain closed-form analytical solutions for equations (2). Therefore, numerical solution is resorted to in this paper. As a first step in this direction the above equations are normalised using the following quantities:

$$T = (T^* - T^*_w)/(T^*_{in} - T^*_w) \quad (3)$$

$$r = (r^* - r^*_w)/r^*_w \quad (4)$$

$$\phi = \phi^*/\beta^* \quad (5)$$

$$Fo = a_1 t/r^{*2}_w \quad (6)$$

$$L = L^*/r^*_w \quad (7)$$

$$W = W^*/r^*_w \quad (8)$$

$$Ste = \pm c_1(T^*_{in} - T^*_w)/\Delta h \quad (+ \text{ freezing}, - \text{ melting}). \quad (9)$$

Even after normalisation the equations involve a time-dependent, moving boundary which is non-concentric and needs a complex book-keeping of a time varying mesh in the computational scheme. This difficulty is circumvented by transforming the equations to a regular and fixed computational domain by using a Landau-type immobilisation parameter [24] defined as:

$$\eta_p = \begin{cases} r/r_f & \text{for } p = 1 \\ (r-L)/(r_f - L) & \text{for } p = 2. \end{cases} \quad (10)$$

The value of η at the moving interface is always unity. The resulting equations are as follows.

Governing equation for PCM:

$$\left(\frac{\partial^2 T}{\partial \eta^2} PRR\right)_p + \left(\frac{\partial T}{\partial \eta} PR\right)_p + \left(\frac{\partial^2 T}{\partial \phi^2} PZZ\right)_p + \left(\frac{\partial T}{\partial \phi} PZ\right)_p + \left(\frac{\partial^2 T}{\partial \eta \partial \phi} PRZ\right)_p = \left(\frac{\partial T}{\partial Fo} PFo\right)_p \quad (11a)$$

$$\text{in } -1 \leqslant \phi \leqslant 1$$

$$p = 1 \text{ in } 0 \leqslant \eta_1 \leqslant 1$$

$$p = 2 \text{ in } 0 \leqslant \eta_2 \leqslant 1.$$

Governing equation for the fin:

$$\left(\frac{\partial^2 T}{\partial \eta^2} FRR\right)_{Fp} + \left(\frac{\partial T}{\partial \eta} FR\right)_{Fp} = \left(\frac{\partial T}{\partial Fo} \frac{a_1}{a_F}\right)_{Fp} + (F)_{Fp} \quad (11b)$$

$$\text{at } \phi = 1, \quad p = 1 \text{ in } 0 \leqslant \eta_1 \leqslant 1$$

$$p = 2 \text{ in } 0 \leqslant \eta_2 \leqslant 1.$$

Boundary conditions:

—at the fin surfaces

$$T_p = T_{Fp} \text{ at } \phi = \pm 1, \quad p = 1 \text{ in } 0 \leqslant \eta_1 \leqslant 1, \quad p = 2 \text{ in } 0 \leqslant \eta_2 \leqslant 1 \quad (11c)$$

—at the insulated periphery

$$\frac{\partial T_{F2}}{\partial \eta_2} = 0 \text{ at } \eta_2 = 0 \quad (11d)$$

$$\frac{\partial T_2}{\partial \eta_2} = \frac{\partial T_2}{\partial \phi} \frac{\phi \tan \alpha^*}{\beta^*(1+L)} (r_f - L) \text{ at } \eta_2 = 0, \quad -1 \leqslant \phi \leqslant 1 \quad (11e)$$

—at the inner tube wall surface

$$T_1 = 0 \text{ at } \eta_1 = 0, \quad -1 \leqslant \phi \leqslant 1 \quad (11f)$$

$$T_{F1} = 0 \text{ at } \eta_1 = 0. \quad (11g)$$

—at the melt/freeze front

$$T_1 = T_2 = T_f \text{ at } -1 \leqslant \phi \leqslant 1, \quad \eta_1 = \eta_2 = 1 \quad (11h)$$

$$\left[-\frac{\lambda_2}{\lambda_1} \frac{\partial T_2}{\partial \eta_2} \frac{1}{(r_f - L)} + \frac{\partial T_1}{\partial \eta_1} \frac{1}{r_f}\right]\left[1 + \frac{\partial r_f}{\partial \phi} \frac{\phi \tan \alpha^*}{\beta^*(1+r_f)}\right] \times \left[1 + \left(\frac{\partial r_f}{\partial \phi} \frac{1}{\beta^*(1+r_f)}\right)^2\right] = \frac{1}{Ste} \frac{\partial r_f}{\partial Fo} \quad (11i)$$

at $\eta_1 = \eta_2 = 1, \quad -1 \leqslant \phi \leqslant 1.$

Initial conditions:

$$T_{F2} = 1 \text{ in } 0 \leqslant \eta_2 \leqslant 1 \tag{11j}$$

$$T_2 = 1 \text{ in } 0 \leqslant \eta_2 \leqslant 1, \quad -1 \leqslant \phi \leqslant 1 \tag{11k}$$

$$r_f = 0 \text{ in } -1 \leqslant \phi \leqslant 1 \tag{11l}$$

where

$$PRR = \left[1 + PZZ\eta^2\left(\frac{\partial r_f}{\partial \phi}\right)^2 - APRZ\eta\frac{\partial r_f}{\partial \phi}\right] \Big/ RF^2 \tag{12}$$

$$PR = \left[\frac{1}{R} + PZZ\eta\frac{2}{RF}\left\{\left(\frac{\partial r_f}{\partial \phi}\right)^2 - \frac{\partial^2 r_f}{\partial \phi^2}\right\} - PZ\eta\frac{\partial r_f}{\partial \phi} - \frac{APRZ}{RF}\frac{\partial r_f}{\partial \phi} + PFo\,\eta\frac{\partial r_f}{\partial Fo}\right] \Big/ RF \tag{13}$$

$$PRZ = \left(-2PZZ\eta\frac{\partial r_f}{\partial \phi} + APRZ\right) \Big/ RF \tag{14}$$

$$PZZ = [1 + (\phi \tan \alpha^*)^2]/(\beta^* R)^2 \tag{15}$$

$$PZ = \phi \tan \alpha^* \left(\sec^2 \alpha^* + \frac{2}{\beta^*}\tan \alpha^*\right) \Big/ (\beta^* R^2) \tag{16}$$

$$APRZ = -2\phi \tan \alpha^*/(\beta^* R) \tag{17}$$

$$PFo = a_1/a_p \tag{18}$$

$$FRR = 1/RF^2 \tag{19}$$

$$FR = \left[AFR + \frac{a_1}{a_F}\eta\frac{\partial r_f}{\partial Fo} + AFC\,\eta\frac{\partial r_f}{\partial \phi}\right] \Big/ RF \tag{20}$$

$$F = AFC\left.\frac{\partial T_p}{\partial \phi}\right|_{\phi = 1} \tag{21}$$

$$AFC = \frac{\lambda_p}{\lambda_F}\frac{1}{R^2}\frac{\sec^2 \alpha^*}{\alpha^* \beta^*} \tag{22}$$

$$AFR = (\alpha^* - \tan \alpha^*)/(R\alpha^*) \tag{23}$$

$$R = \begin{cases} 1 + \eta_1 r_f & \text{for } p = 1 \\ 1 + L + \eta_2(r_f - L) & \text{for } p = 2 \end{cases} \tag{24}$$

$$RF = \begin{cases} r_f & \text{for } p = 1 \\ (r_f - L) & \text{for } p = 2 \end{cases} \tag{25}$$

$$\alpha^* = \sin^{-1}(W/2R) \tag{26}$$

$$\beta^* = \frac{\pi}{N} - \alpha^*. \tag{27}$$

ENERGY ACCOUNT

Since this paper is concerned with LHTES applications, evaluation of the energy transferred is as important as tracking the moving interface. The amount of energy stored/discharged up to any given instant can be computed by calculating the enthalpy change of the PCM–fin assembly. For comparison purposes the energy transfer is normalised using a factor E^* defined below:

$$E^* = \pm \pi r_w^{*2}(\rho c)_1 (T_{in}^* - T_w^*) \tag{28}$$

(+freezing, −melting).

The resulting dimensionless term can be designated as energy density. The various energy density components contributing to the total energy density are as follows:

$$E1 = \frac{N}{\pi}\frac{a_1}{a_2}\frac{\lambda_2}{\lambda_1}(1 - T_f) \times \int_{\phi=-1}^{+1}\int_{\eta_1=0}^{1} \beta^* r_f(1 + \eta_1 r_f)\,d\eta_1\,d\phi \tag{29}$$

$$E2 = \frac{N}{\pi}\frac{1}{Ste}\int_{\phi=-1}^{+1}\int_{\eta_1=0}^{1} \beta^* r_f(1 + \eta_1 r_f)\,d\eta_1\,d\phi \tag{30}$$

$$E3 = \frac{N}{\pi}\int_{\phi=-1}^{+1}\int_{\eta_1=0}^{1} \beta^* r_f(1 + \eta_1 r_f)(T_f - T_1)\,d\eta_1\,d\phi \tag{31}$$

$$E4 = \frac{N}{\pi}\frac{a_1}{a_2}\frac{\lambda_2}{\lambda_1}\int_{\phi=-1}^{+1}\int_{\eta_2=0}^{1} [\beta^*(L - r_f) \times \{1 + L + \eta_2(r_f - L)\}(1 - T_2)]\,d\eta_2\,d\phi \tag{32}$$

$$E5 = \frac{N}{\pi}\frac{2a_1}{a_F}\frac{\lambda_F}{\lambda_1}\int_{\eta_1=0}^{1} \alpha^* r_f(1 + \eta_1 r_f)(1 - T_{F1})\,d\eta_1 \tag{33}$$

$$E6 = \frac{N}{\pi}\frac{2a_1}{a_F}\frac{\lambda_F}{\lambda_1}\int_{\eta_2=0}^{1} \alpha^*(L - r_f) \times \{1 + L + \eta_2(r_f - L)\}(1 - T_{F2})\,d\eta_2 \tag{34}$$

where $E1$ is the sensible heat transferred in changing the temperature of phase 1 of PCM in the region $r_f^* \geqslant r^* \geqslant r_w^*$ from the initial temperature T_{in}^* to its phase-change temperature T_f^*; $E2$ is the latent heat transferred in changing the phase of the PCM in the region $r_f^* \geqslant r^* \geqslant r_w^*$; $E3$ is the sensible heat of phase 1 of PCM in the region $r_f^* \geqslant r^* \geqslant r_w^*$ measured from its phase-change temperature T_f^* to the temperature T_1^*; $E4$ is the sensible heat change in phase 2 of PCM in the region $(r_w^* + L^*) \geqslant r^* \geqslant r_f^*$, measured from the initial temperature T_{in}^*; $E5$ is the sensible heat of fin adjoining phase 1 of PCM, in the region $r_f^* \geqslant r^* \geqslant r_w^*$, reckoned from the initial temperature T_{in}^*; and $E6$ is the sensible heat of fin adjoining phase 2 of PCM, in the region $(r_w^* + L^*) \geqslant r^* \geqslant r_w^*$ with reference to the initial temperature T_{in}^*.

The total energy density is given by

$$ET = E1 + E2 + E3 + E4 + E5 + E6. \tag{35}$$

The charging/discharging of energy continues till the entire finned tube–PCM assembly reaches a steady-state temperature of T_w^* (at which time all the PCM is in phase 1). Therefore, the steady-state energy density is also the maximum possible energy density

EM given by the equation

$$EM = \frac{N}{\pi}\left[WL\frac{a_1}{a_F}\frac{\lambda_F}{\lambda_1} + \frac{\pi}{N}\left\{(1+L)^2 - 1 - \frac{NWL}{\pi}\right\} \times \left\{\frac{a_1}{a_2}\frac{\lambda_2}{\lambda_1}(1-T_f) + \frac{1}{Ste} + T_f\right\}\right]. \quad (36)$$

The volume of fin space per unit volume of the cylindrical annulus is expressed quantitatively by the factor fin content (FC) defined as:

$$FC = \frac{N}{\pi}\frac{WL}{[(1+L)^2-1]}. \quad (37)$$

The ratio of heat transfer area of the finned annulus to that of the unfinned annulus is specified by the area factor (AF)

$$AF = 1 + \frac{N}{\pi}(L - W/2). \quad (38)$$

The volume of PCM that has undergone phase change per unit volume of the finned annulus–PCM assembly is defined as phase-change fraction VF which is evaluated by the following expression

$$VF = \frac{N}{\pi[(1+L)^2-1]}\int_{\phi=-1}^{1}\int_{\eta_1=0}^{1} r_f\beta^* \times (1+\eta_1 r_f)\,d\eta_1\,d\phi. \quad (39)$$

COMPUTATIONAL PROCEDURE

A starting solution is needed for the finite-difference scheme, as phase 1 of the PCM is non-existent at zero time. A starting value (at the end of the first time step) for the phase front thickness is assumed to be equal to that given by Neumann's solution [25] for phase change in a semi-infinite planar body. Then the phase front thickness at the first time step is

$$r_f = 2p(Fo)^{1/2} \quad (40)$$

where p is the root of the transcendental equation

$$T_f - \frac{\lambda_2}{\lambda_1}\left(\frac{a_1}{a_2}\right)^{1/2}(1-T_f)\left\{\operatorname{erf}(p)\exp\left[p^2\left(1-\frac{a_1}{a_2}\right)\right] \div \operatorname{erfc}\left[p\left(\frac{a_1}{a_2}\right)^{1/2}\right]\right\} = \frac{p\pi^{1/2}\operatorname{erf}(p)\exp(p^2)}{Ste}. \quad (41)$$

The phase front profile is assumed to be concentric at the first time step. The fin equation (11b) is then solved neglecting the PCM temperature gradients in the ϕ direction, to get the fin temperature profile. The PCM temperature profile is assumed to be the same as that of the fin, at all the ϕ planes. This completes the starting solution.

A formal solution of the governing equations is then obtained using an adaptation of the Alternating Direction Implicit (ADI) method as outlined below.

Following a quasi-stationary approach, the phase front profile at the new time level is obtained by explicitly solving equation (11i). The fin equation (11b) and the PCM equation (11a) are then solved implicitly, in that order, to obtain the temperature profiles in the fin and PCM, respectively, at the new time level. The mixed derivatives are treated as known quantities and evaluated from the values of variables at the previous time step in order to retain the tri-diagonal nature of the difference equations. Further details of the finite-difference scheme can be found elsewhere [26].

The solution of the problem is stopped at the instant the phase front reaches the fin tip, as the space domains specified in equations (2) and (11) lose their validity beyond this time. This time will hereafter be referred to as process time. Beyond the process time, the fins exchange heat with only phase 1 of PCM. Phase-change process beyond the process time is a separate problem by itself with the initial conditions being those prevailing at the end of process time. Such a solution, beyond the process time is not considered in this paper.

A space step size of $\Delta\eta_1 = \Delta\eta_2 = \Delta\phi = 0.1$ is uniformly used in all the computations. The time step size is chosen by trial and error and a range of $\Delta Fo = 0.002$ to 0.05 is found to be satisfactory for the range of parameters considered in this paper.

The number of fins is a critical parameter in the selection of a suitable time step, with a larger N value requiring a smaller step. Too large a time step gives rise to wiggles in the interface profile.

The various energy components are evaluated by numerical integration using the trapezoidal rule.

RESULTS AND DISCUSSION

As a specific example, the melting/freezing of paraffins in a cylindrical annulus with copper fins is analysed. Typical properties of these materials are listed in Table 1. The following parameters are used in the analysis, except where otherwise specified.

$$Ste = 0.5, \quad N = 4, \quad a_1/a_2 = \lambda_2/\lambda_1 = 1$$
$$T_f = 0.8, \quad L = 1.5, \quad a_1/a_F = 8\times10^{-4}$$
$$W = 0.1, \quad \lambda_1/\lambda_F = 4\times10^{-4}.$$

This gives a fin content of 0.036 with a heat transfer area factor of 2.846.

The shape of the moving interface at different times is shown in Fig. 2.

Figure 3 shows the variation of the various energy components. It is seen that the latent heat is the major contributor (about 70%) to the energy storage density. Only 20% is contributed by the sensible heat of PCM and the balance by the sensible heat of the fin.

While the components $E1$, $E2$, $E3$, $E5$ all increase with time, the sensible heat of the unmolten/unfrozen PCM, $E4$ and that of the fin, $E6$ initially increase with

Table 1. Thermophysical properties

S. no.	Properties	Units	Water [27] Liquid	Water [27] Solid	*n*-Eicosane [28] Liquid	*n*-Eicosane [28] Solid	Copper [27]
1.	Saturation temperature	°C	0		36.4		—
2.	Latent heat	kJ kg^{-1}	333		247		—
3.	Density	kg m^{-3}	1000	917	778	856	8300
4.	Thermal conductivity	W m^{-1} K^{-1}	0.552	2.250	0.150	0.150	372
5.	Specific heat	kJ kg^{-1} K^{-1}	4.220	2.040	2.010	2.210	0.419
6.	Thermal diffusivity ($\times 10^6$)	m^2 s^{-1}	0.143	1.2	0.096	0.079	107

time, reach a peak and then start decreasing. In the initial stages the change in temperature of phase 2 is dominant and at later times the reduction in the size of the unmolten/unfrozen region is dominant.

The effect of Stefan number on the total energy density ET and the phase-change fraction VF is shown in Fig. 4. Phase-change fraction VF is lower for smaller Stefan numbers indicating that the melting/freezing rate is slower. This is due to the fact that either the latent heat is large or the driving force $\pm(T^*_{in} - T^*_w)$ is small for low values of Ste. Necessarily the phase-change process is slowed down at lower values of Ste.

However, the total energy density shows an upward swing for lower values of Ste. Hence for LHTES, low Stefan number is desirable.

The effect of T_f is displayed in Fig. 5. The smaller the value of T_f, the smaller is the phase-change fraction VF. Smaller T_f means that the initial temperature T^*_{in} is far different from that of the PCM phase-change temperature T^*_f. So the result that the phase-change fraction is higher for $T_f = 1$ is only to be expected, as no energy is utilised for the parasitic sensible heating/cooling of phase 2 of the PCM.

For times greater than $Fo = 1.0$, the energy density curves are similar to phase-change fraction curves with smaller T_f values giving smaller energy densities. But for times $Fo < 1.0$, the converse is noticed.

It is also seen that the total energy density and the phase-change fraction at the instant the fin tip is reached by the interface, is nearly the same, within the range of T_f values considered.

Broadly speaking, for LHTES applications, it is desirable to have the initial PCM temperature at the

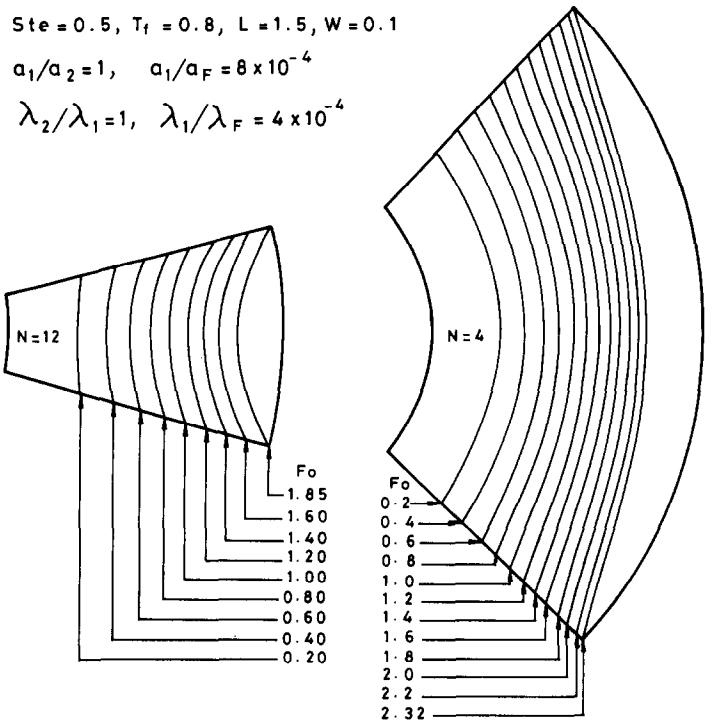

FIG. 2. Timewise evolution of the frozen/molten layer.

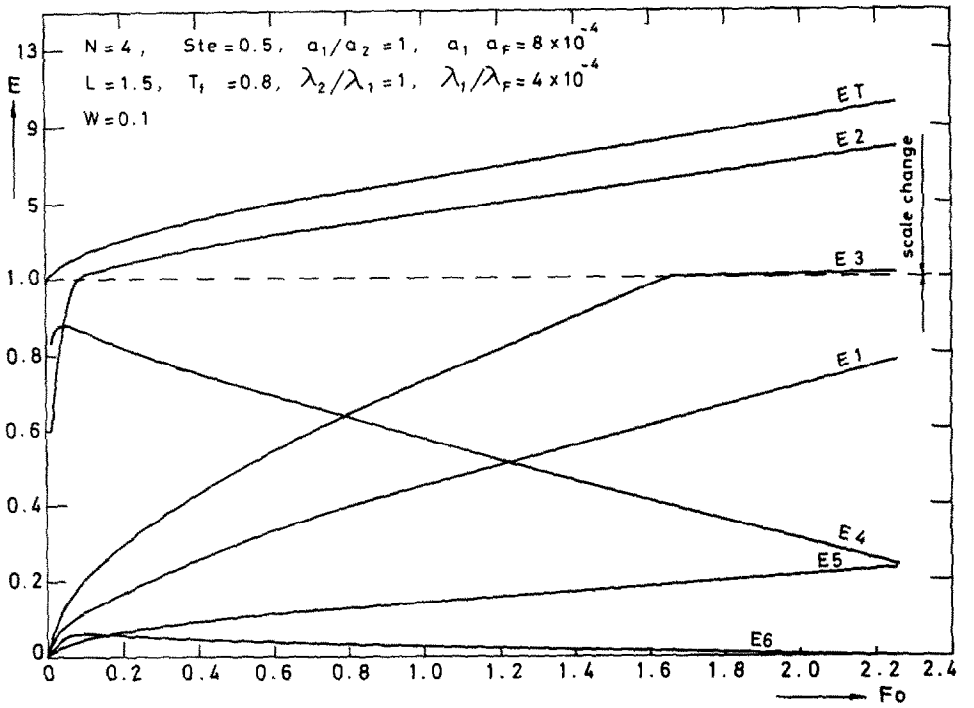

FIG. 3. Temporal variation of energy components.

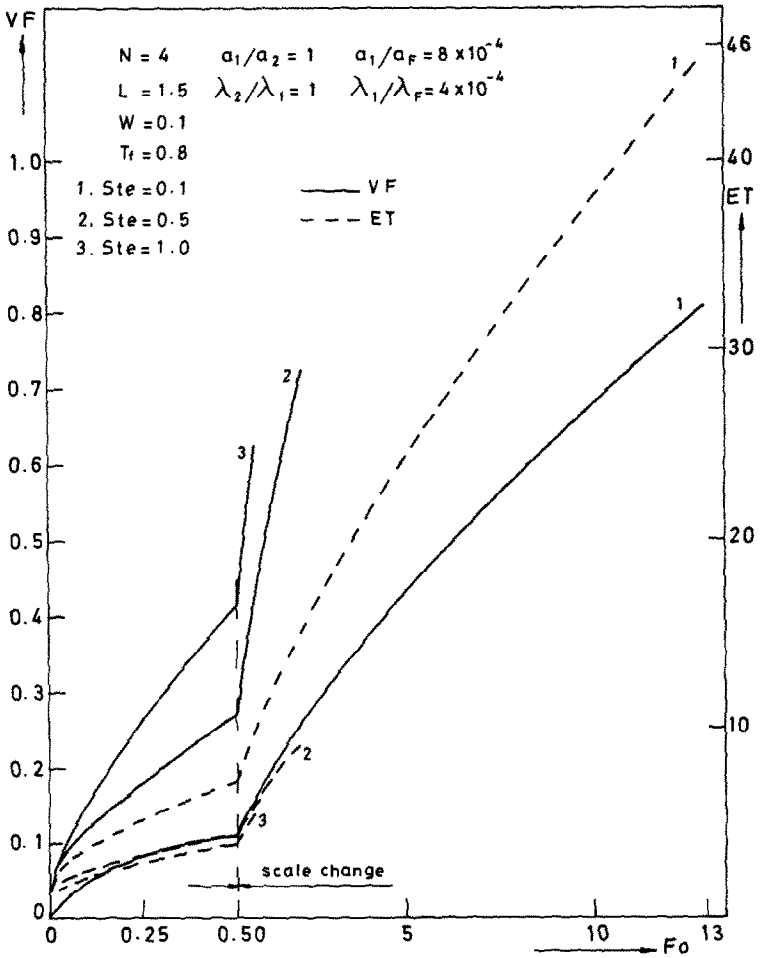

FIG. 4. Effect of *Ste* on *VF* and *ET*.

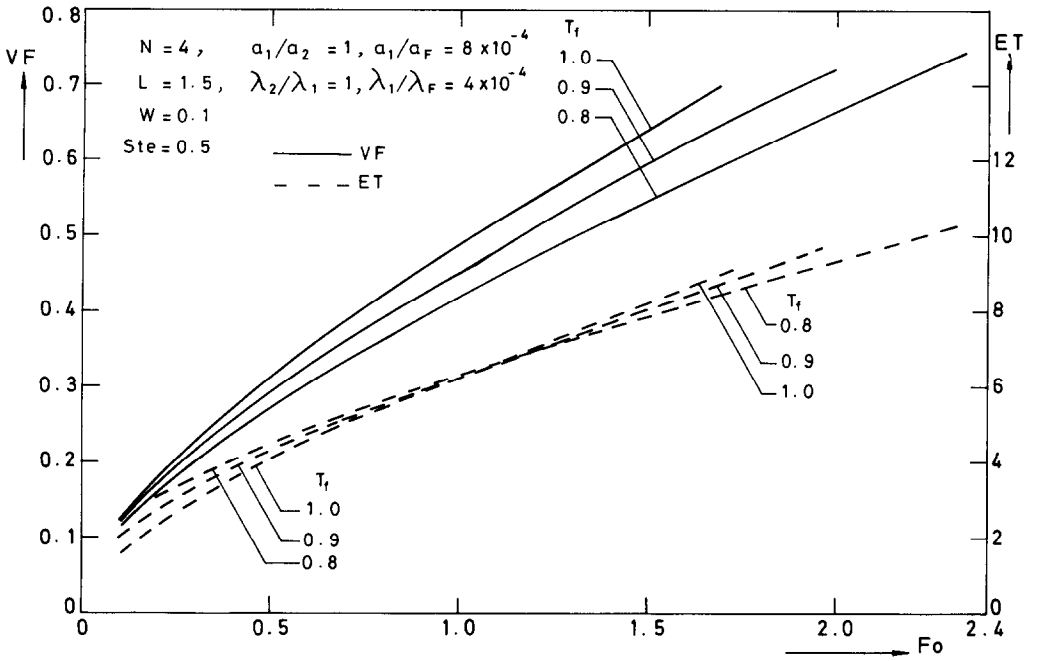

FIG. 5. Effect of T_f on VF and ET.

saturation value. This however is difficult to achieve even in laboratory conditions and more so in the field. A value of $T_f = 0.8$ may be taken as a realistic value for LHTES devices.

The effect of the number of fins N around the cylinder is shown in Fig. 6. The phase-change fraction VF and the total energy density ET are greater at any given time, for a large number of fins.

Analysis of phase change in an unfinned annulus as presented by Sinha and Gupta [29] has been repeated for the PCM under consideration and the results are plotted in Fig. 6 for comparison purposes. Even a single finned annulus is found to be superior to the unfinned annulus. It must be remembered that both the fin content and heat transfer area factor linearly increase with the number of fins, the latter increasing at a faster rate for the values of W and L used in the analysis.

The phase-change fraction at the end of the process is almost constant irrespective of the number of fins used within the range of the parametric analysis. But the process time decreases with an increase in the number of fins.

The number of fins cannot be increased beyond a maximum value of $2\pi/W$. However, the actual number of fins will also have to be decided by the PCM content and the phase-change fraction. For example, with $W = 0.1$, the maximum number of fins possible is 62 which gives a fin content of 0.564 for $L = 1.5$. This reduces the available space for the PCM considerably and hence the phase-change fraction cannot exceed a value of 0.436 which is well below the value of 0.8 obtained with N in the range of 1 to 12.

Figure 7 shows the effect of the fin thickness W on the total energy density and the phase-change fraction. With an increase in W, the phase-change fraction and the total energy density are lower. This is because the fin content decreases appreciably, while there is a small increase in heat transfer area when thin fins are used. Therefore it is desirable to have thin fins for better performance in LHTES.

It is seen in Fig. 8 that decreasing the fin length L (i.e. decreasing the outer radius of the annulus) gives very high values of VF at any given time, apparently indicating a marked improvement in the performance. This improvement is illusory, as VF by definition is per unit volume of the PCM–finned annulus assembly. A true picture is given by the plot of $VF[(1+L)^2-1]$ which shows that the phase-change volume at any instant is virtually unaffected by the choice of L.

The plot of ET shows that the energy transfer is greater for larger fin lengths, at any given time. More important is the fact that the value of ET at the end of the process, increases enormously with increasing L. Hence larger fin lengths are desirable.

The effect of the ratio of the thermal conductivity of PCM to that of fin is seen in Fig. 9. The value of λ_1/λ_F has negligible effect on the phase-change fraction. The total energy density slightly increases with decreasing λ_1/λ_F indicating that a good conductor is preferable as fin material. It can also be interpreted to mean that for poor conductivity PCMs, it is advantageous to use fins. The process time, final energy density and final phase-change fraction are not significantly affected by the ratio λ_1/λ_F.

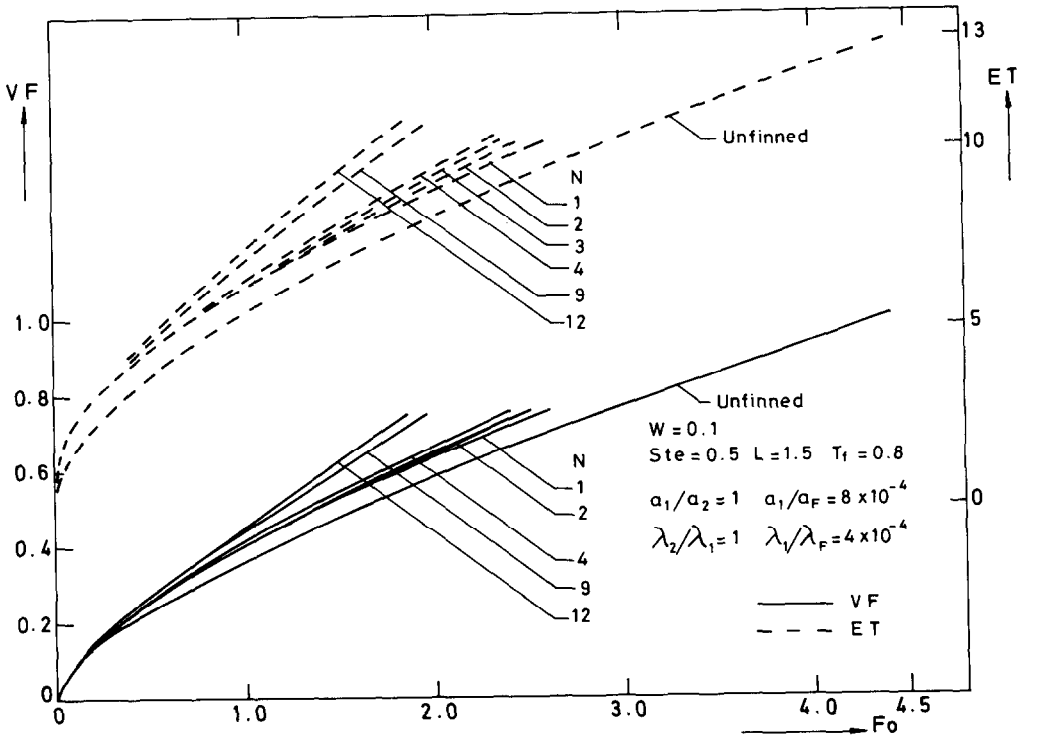

FIG. 6. Effect of the number of fins on *VF* and *ET*.

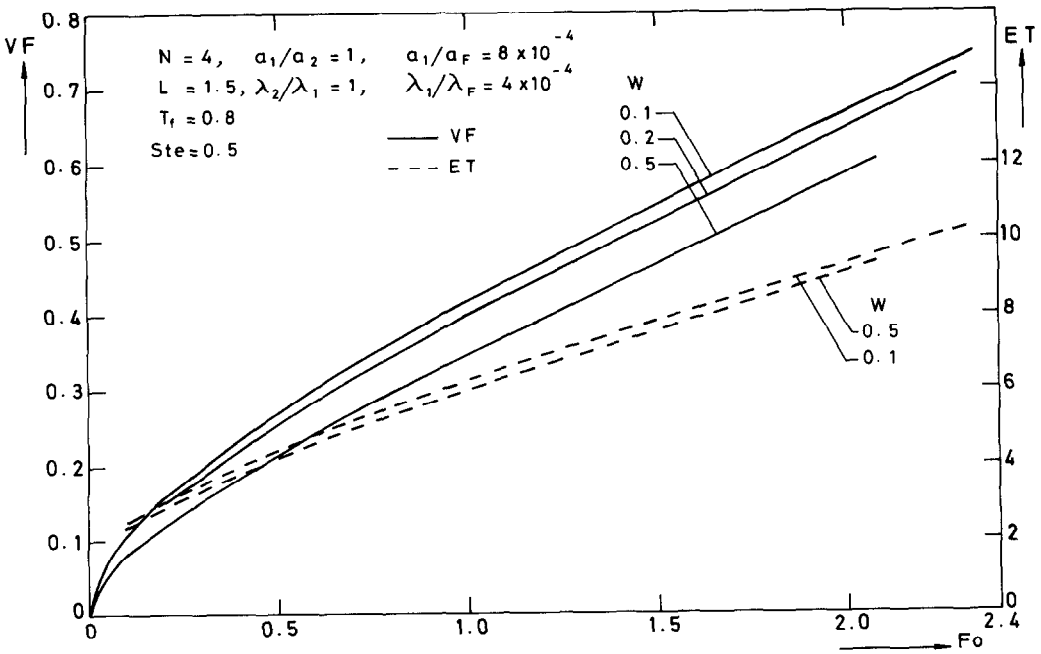

FIG. 7. Effect of fin thickness on *VF* and *ET*.

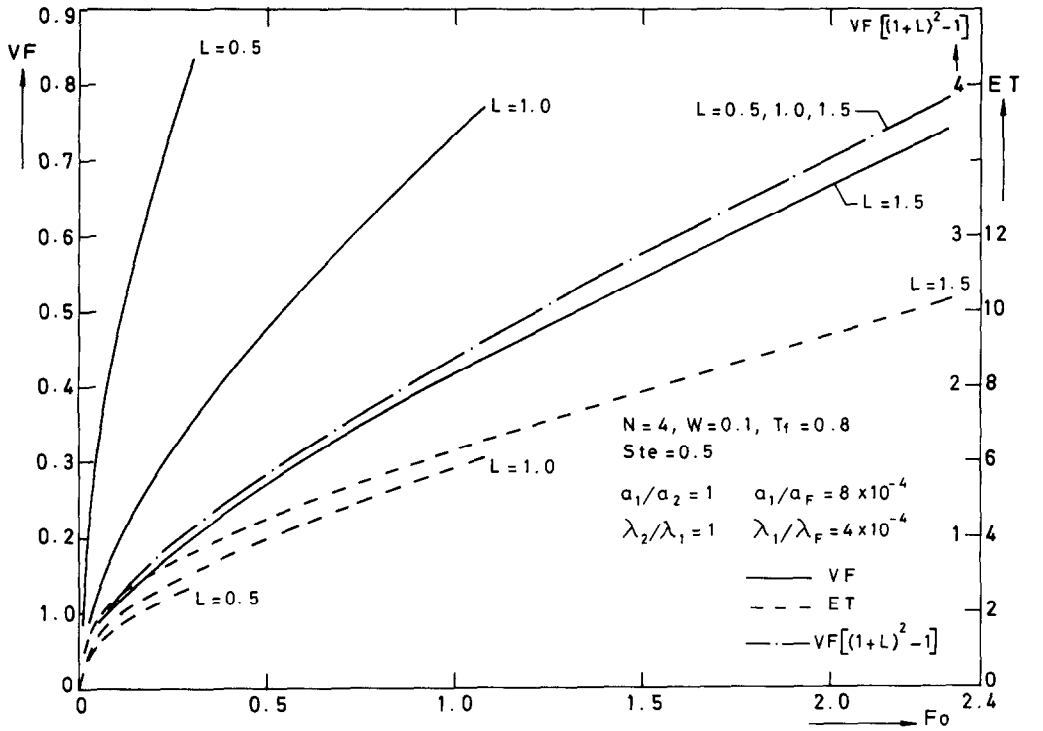

FIG. 8. Effect of fin length on *VF* and *ET*.

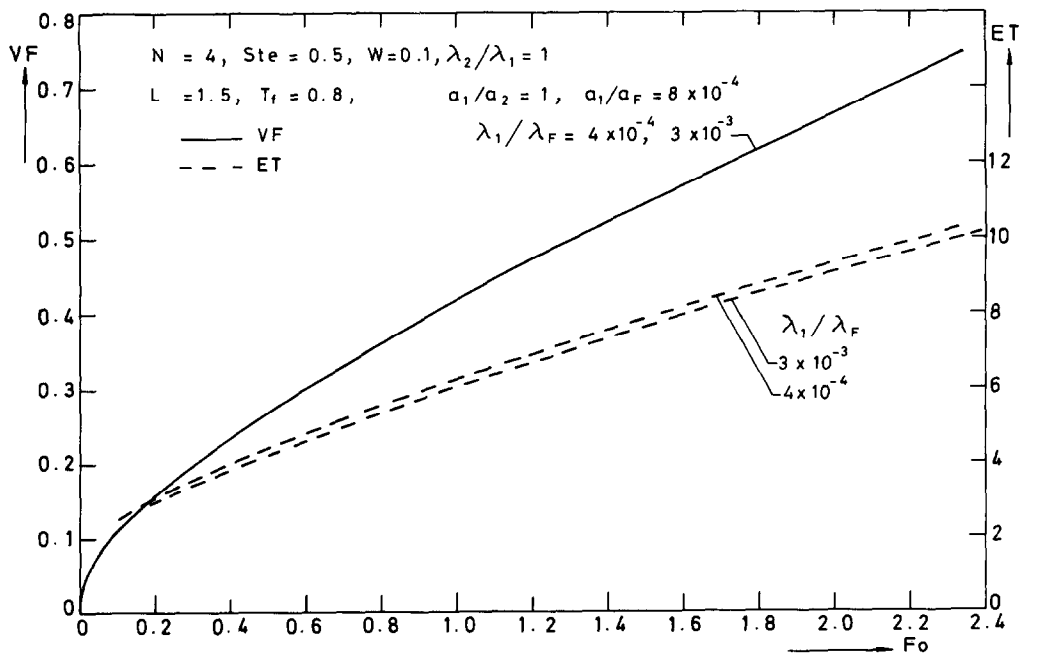

FIG. 9. Effect of λ_1/λ_F on *VF* and *ET*.

The ratio of diffusivity of the PCM to that of the fin (a_1/a_F) has virtually no effect on the phase-change fraction as seen in Fig. 10. Higher values of a_1/a_F give marginally greater values of total energy density. It does not cause appreciable changes in the process time, final energy density and final phase-change fraction.

Figure 11 shows that the ratio of the thermal conductivities between the two phases of PCM (λ_2/λ_1), while significantly affecting the energy density, has virtually no effect on phase-change fraction. Larger values of λ_2/λ_1 produce greater energy densities. Total process time is not significantly affected by the ratio λ_2/λ_1.

It is seen from Fig. 12 that larger thermal diffusivity ratio, a_1/a_2, produces larger total energy density at any given instant. It has negligible effect on the phase-change fraction at any given instant and the total process time.

Though large values of a_1/a_2 and λ_2/λ_1 are advantageous in LHTES devices, the choice of PCM is likely to be influenced by other factors like the phase-change temperature T_f^*, latent heat Δh, thermal cycling behaviour, etc.

Sparrow *et al.*'s [18] finned tube experiments with an initially saturated PCM showed that the phase-change fraction can be estimated by the relation

$$VF \propto (Fo\ Ste\ T_f)^{0.5}. \tag{42}$$

It is seen in the present analysis that VF is a strong function of system geometry parameters (N, L and W). As already pointed out, the material property ratios λ_2/λ_1, a_1/a_2, λ_1/λ_F and a_1/a_F do not affect VF significantly. A working equation arrived at for the phase-change fraction through a multiple regression analysis of nearly 150 data points obtained from the results of the present analysis is given below

$$VF = 1.1275(Fo\ Ste\ T_f)^{0.624}\ (N)^{0.028}\ (L)^{-1.385}\ (W)^{-0.049}. \tag{43}$$

The correlation is represented graphically in Fig. 13. The standard error of estimate for the above correlation is 0.07 and is accurate enough for engineering design purposes, in the range of parameters given below:

$$Ste = 0.1\text{–}1.0, \quad \lambda_1/\lambda_F = 4\times10^{-4}\text{–}3\times10^{-3}$$
$$T_f = 0.8\text{–}1.0, \quad a_1/a_F = 8\times10^{-4}\text{–}2.5\times10^{-3}$$
$$W = 0.1\text{–}0.5, \quad \lambda_2/\lambda_1 = 0.5\text{–}1.5$$
$$L = 0.5\text{–}1.5, \quad a_1/a_2 = 0.5\text{–}1.5$$
$$N = 1\text{–}12.$$

CONCLUDING REMARKS

Analysis of phase change around an axially finned annulus indicates that the addition of fins is advantageous for energy storage applications.

From the storage point of view the fins should be long and thin and should be made of good thermal conductors. The PCM should have a large latent heat and should be initially near to its saturation temperature as far as possible.

The melt/frozen fraction is a weak function of λ_2/λ_1, λ_1/λ_F, a_1/a_2 and a_1/a_F and can be estimated from the working equation

$$VF = 1.1275(Fo\ Ste\ T_f)^{0.624}\ (N)^{0.028}\ (L)^{-1.385}\ (W)^{-0.049}.$$

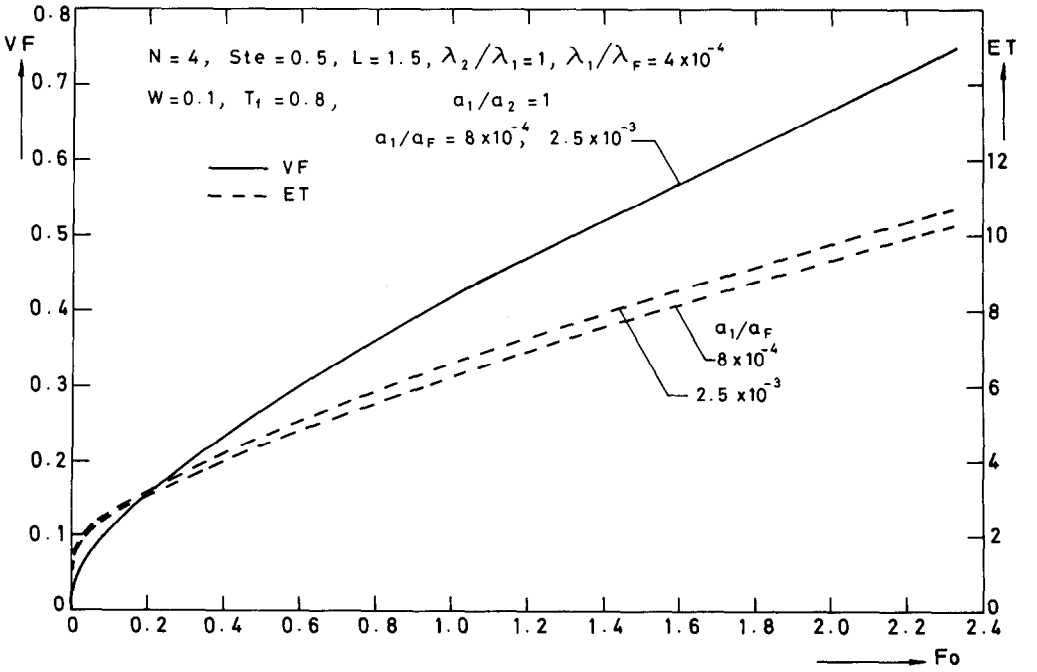

FIG. 10. Effect of a_1/a_F on VF and ET.

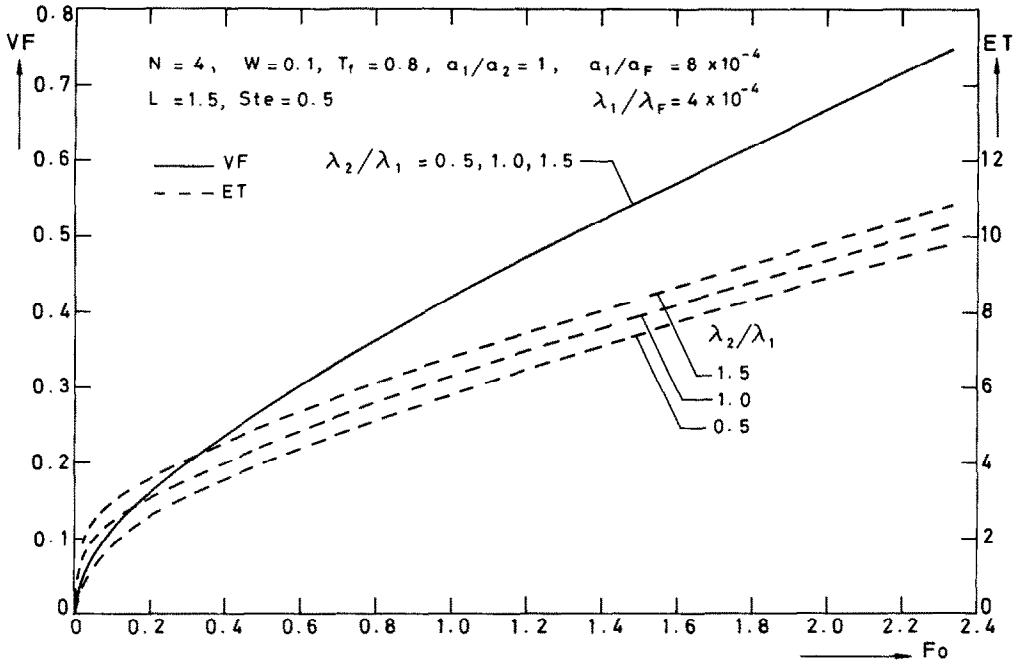

FIG. 11. Effect of λ_2/λ_1 on *VF* and *ET*.

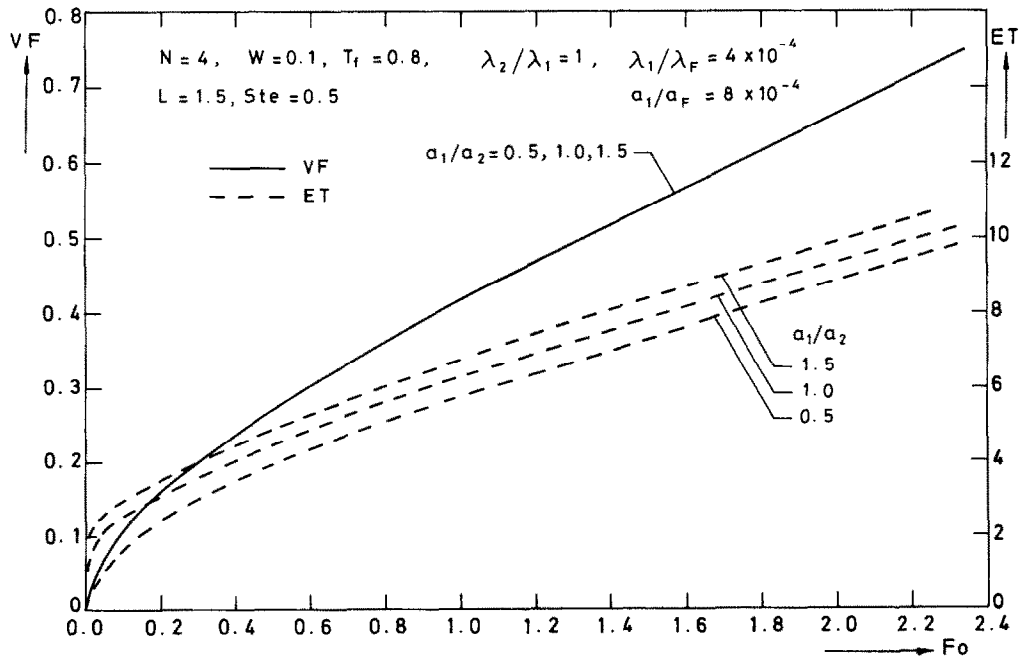

FIG. 12. Effect of a_1/a_2 on *VF* and *ET*.

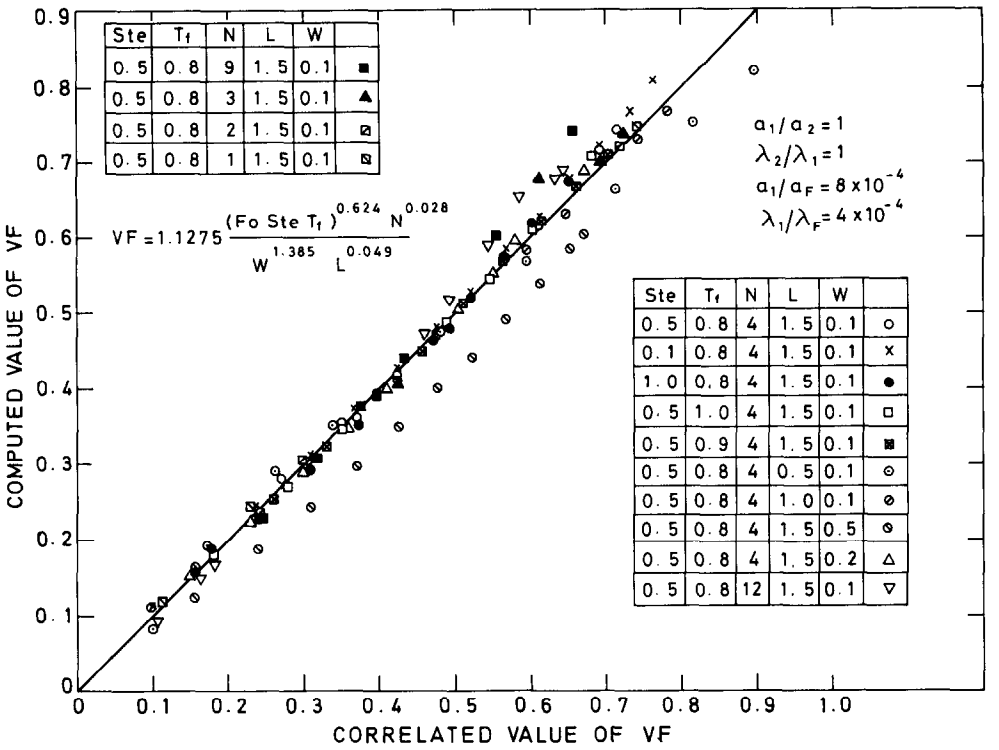

FIG. 13. Correlation for phase-change fraction as a function of fin parameters.

REFERENCES

1. R. T. Lefrois and A. K. Mathur, Active heat exchanger evaluation for latent heat thermal energy storage systems, ASME paper 82-HT-7 (1982).
2. C. S. Herrick, Melt-freeze-cycle life-testing of Glauber's salt in a rolling cylinder heat store, *Sol. Energy* **28**, 99–104 (1982).
3. D. D. Edie and S. S. Melsheimer, An immiscible fluid-heat of fusion energy system, *Proc. ISES Congress, Sharing the Sun: Solar Technology in the Seventies* (Edited by K. W. Boer), Vol. 8, pp. 262–272 (1976).
4. D. D. Edie, S. S. Melsheimer, J. J. Mullins and J. F. Marra, Latent heat storage using direct contact heat transfer, *Proc. ISES Congress, SUN II* (Edited by K. W. Boer and B. H. Glenn), Vol. I, pp. 640–644 (1979).
5. A. D. Mills, S. S. Melsheimeer and D. D. Edie, Extended cycling behaviour of a direct contact-phase change TES system, *A.I.Ch.E. Symp. Ser.* **198**(76), 41–46 (1980).
6. A. E. Fouda, G. J. G. Despault, J. B. Taylor and C. E. Capes, Solar storage systems using salt hydrate latent heat and direct contact heat exchange—I. Preliminary design considerations, *Sol. Energy* **25**, 437–444 (1980).
7. M. E. Cease, A model of direct contact heat transfer for latent heat energy storage, *Proc. 15th IECE Conference*, Vol. I, pp. 624–629 (1980).
8. J. E. Helshoj, A high-capacity, high-speed latent heat storage unit, *Proc. ISES Congress*, Brighton, *Solar World Forum*, Vol. I, pp. 703–709 (1982).
9. E. M. Mehalik and A. T. Tweedie, Two component thermal energy material, NSF report NSF/RANN/SE/AER 74-09186 (1975).
10. E. van Galen and C. den Ouden, Development of a storage system based on encapsulated p-c materials, *Proc. ISES Congress, SUN II* (Edited by K. W. Boer and B. H. Glenn), Vol. I, pp. 655–658 (1979).
11. J. Chen, Pelletisation and roll encapsulation of thermal energy storage materials, *Proc. 16th IECE Conference*, Vol. 1, pp. 931–934 (1981).
12. P. A. Bahrami, Fusible pellet transport and storage of heat, ASME paper 82-HT-32 (1982).
13. W. R. Humphries and E. I. Griggs, A design handbook for phase change thermal control and energy storage devices, NASA Report TP 1074 (1977).
14. R. N. Smith, T. E. Ebersole and F. P. Griffin, Heat exchanger performance in latent heat thermal energy storage, *J. Sol. Energy Engng* **102**, 112–118 (1980).
15. J. Eftekhar, A. Haji-Sheik and D. Y. S. Lou, Heat transfer enhancement in a paraffin wax thermal storage system, *Proc. ASME Solar Energy Conference* (Edited by L. M. Murphy), pp. 45–52 (1983).
16. H. C. Maru, A. Kardas, V. M. Huang, J. F. Dullea, L. Paul and L. G. Marianowski, Molten salt thermal energy storage systems, Institute of Gas Technology, Chicago, IL, Report UC-94A (1978).
17. A. Abhat, Experimentation with a prototype latent heat thermal energy storage system, *Proc. ISES Congress, SUN II* (Edited by K. W. Boer and B. H. Glenn), Vol. I, p. 659 (1979).
18. E. M. Sparrow, E. D. Larson and J. W. Ramsey, Freezing on a finned tube for either conduction-controlled or natural-convection-controlled heat transfer, *Int. J. Heat Mass Transfer* **24**, 273–284 (1981).
19. A. C. Bathelt and R. Viskanta, Heat transfer and interface motion during melting and solidification around a finned heat source/sink, *J. Heat Transfer* **103**, 720–726 (1981).
20. A. Abhat, S. Aboul-Enein and N. A. Malatidis, Heat of fusion storage systems for solar heating applications, *Proc. Int. TNO-Symposium*, Amsterdam (Edited by C. den Ouden), pp. 151–171 (1981).
21. K. J. Mody, Solar energy storage subsystem utilising latent

heat of phase change. Ph.D. Thesis, North Carolina State University (1977).
22. R. H. Henze and J. A. C. Humphrey, Enhanced conduction in phase change thermal energy storage devices, *Int. J. Heat Mass Transfer* **24**, 459–473 (1981).
23. A. Abhat, S. Aboul-Enein and N. A. Malatidis, Latent heat thermal energy storage—determination of properties of storage media and development of a new heat transfer system, Final report, EG Contract No. 643-78-7 ESD, IKE, Stuttgart, F.R.G. (1980).
24. H. G. Landau, Heat conduction in a melting solid, *Q. appl. Math.* **8**, 81–84 (1950).
25. H. S. Carslaw and J. C. Jaeger, *Conduction of Heat in Solids*. Clarendon Press, Oxford (1959).
26. P. V. Padmanabhan, Studies on direct contact and extended surface heat transfer with phase change for thermal energy storage. Ph.D. thesis, Indian Institute of Technology, Madras (1985).
27. U. Grigull and H. Sandner, *Heat Conduction*. Hemisphere, Washington, DC (1984).
28. A. D. Solomon, An easily computable solution to a two phase Stefan problem, *Sol. Energy* **23**, 525–528 (1979).
29. T. K. Sinha and J. P. Gupta, Solidification in an annulus, *Int. J. Heat Mass Transfer* **25**, 1771–1773 (1982).

CHANGEMENT DE PHASE DANS UN ESPACE ANNULAIRE CYLINDRIQUE AVEC DES AILETTES AXIALES SUR LE TUBE INTERNE

Résumé—Une analyse théorique est présentée pour le changement de phase dans un anneau cylindrique dans lequel des ailettes rectangulaires, uniformément espacées sont attachées au tube intérieur isotherme, tandis que le tube externe est adiabatique. Le modèle suppose que la conduction est le seul mode de transfert. Les équations sont résolues par des méthodes aux différences finies. On présente l'évolution dans le temps du profil de l'interface, de la fraction de phase et du rapport énergies stockée/libérée et de l'effet des neuf paramètres descriptifs. A partir de l'analyse, on propose une formule pratique pour les ingénieurs :

$$VF = 1{,}1275\ (Fo\ Ste\ T_f)^{0.624}\ (N)^{0.028}\ (L)^{-1.385}\ (W)^{-0.049}.$$

PHASENÄNDERUNGEN IN EINEM ZYLINDRISCHEN RINGSPALT MIT AXIALEN RIPPEN AUF DEM INNENROHR

Zusammenfassung—Eine theoretische Untersuchung wird vorgelegt für den Phasenänderungsprozeß in einem zylindrischen Ringspalt, wobei rechteckige, gleichförmig angebrachte axiale Rippen auf dem inneren isothermen Rohr im Ringspalt befestigt sind, während das Außenrohr adiabat gehalten wird. Das Modell betrachtet die Wärmeleitung als einzigen Wärmeübertragungs-Mechanismus. Die Bilanzgleichungen werden mit Differenzenverfahren gelöst. Der zeitliche Verlauf der Phasengrenzen, des Anteils der Phasen, der ein-/ausgespeicherten Energie und der Einfluß aller neun bestimmenden Parameter wird aufgezeigt. Aus der Untersuchung wird eine Arbeitsgleichung für ingenieurmäßige Auslegungsberechnungen vorgeschlagen:

$$VF = 1{,}1275\ (Fo\ Ste\ T_f)^{0.624}(N)^{0.028}(L)^{-1.385}(W)^{-0.049}.$$

ФАЗОВЫЕ ПРЕВРАЩЕНИЯ В ЦИЛИНДРИЧЕСКОМ КОЛЬЦЕВОМ КАНАЛЕ С ОСЕВЫМИ РЕБРАМИ НА ВНУТРЕННЕЙ ТРУБЕ

Аннотация—Выполнен теоретический анализ процесса фазового превращения в цилиндрическом кольцевом канале, в котором прямоугольные, равномерно расположенные осевые ребра прикреплены к внутренней изотермической трубе, в то время как наружная труба поддерживалась адиабатической. В модели предполагается, что единственным механизмом теплопереноса является теплопроводность. Определяющие уравнения решены методом конечных разностей. Представлены развивающиеся во времени пограничные профили, доля фазового превращения и запасаемая/отдаваемая энергия, а также эффекты всех девяти параметров. Предложена формула для инженерных расчетов.